Estimation of lateral-directional aerodynamic derivatives from flight data using conventional and neural based methods

R. Kumar
rakpec@gmail.com
Department of Aerospace Engineering
PEC University of Technology, Sector-12
Chandigarh
India

A. K. Ghosh
akg@iitk.ac.in
Department of Aerospace Engineering,
Indian Institute of Technology
Kanpur
India

ABSTRACT

The paper presents the estimation of lateral-directional aerodynamic derivatives (parameters) using conventional and neural based methods from real flight data of Hansa-3 aircraft. The conventional methods such as least squares (LS) and maximum likelihood (ML) require an a priori postulation of mathematical model to estimate the parameters. Whereas the neural-based method such as Neural-Gauss-Newton (NGN) is an algorithm that utilises feed forward neural network and Gauss-Newton optimisation to estimate the parameters and does not require any a priori postulation of mathematical model or solution of equations of motion. In the paper, the LS, ML and NGN methods are applied to lateral-directional flight data in order to estimate parameters. The results obtained in terms of lateral-directional aerodynamic derivatives are reasonably accurate to establish LS, ML and NGN as parameter estimation methods along with NGN method having an additional

Paper No. 4011. Manuscript received 2 June 2013, revised version received 1 March 2014, accepted 10 June 2014.

https://doi.org/10.1017/S0001924000010149 Published online by Cambridge University Press

advantage of non-requirement of a priori mathematical model. The paper also highlights the effect of different types of control inputs on parameter estimation. For this, three types of control inputs were used to generate real flight data. The ailerons and rudder were deflected in the first, the ailerons were deflected while keeping rudder at trim condition in the second and the rudder was deflected while keeping ailerons at trim condition in the third type of control input to generate the real flight data. The paper presents the effect of three different types of control inputs in terms of aerodynamic parameters estimated through conventional and neural based methods using flight data generated through these inputs.

NOMENCLATURE

a_x, a_y, a_z	linear accelerations along x-, y- and z-body axes, respectively (ms^{-2})
b	wing span (m)
C_l, C_n	rolling and yawing moment coefficients, respectively
C_{l_0}, C_{n_0}	rolling and yawing moment coefficients at zero angle of attack, respectively
C_Y	side force coefficient
$\bar{c}$	mean aerodynamic chord (m)
g	acceleration due to gravity (ms^{-2})
I_x, I_y, I_z	moment of inertia about x, y and z-axis, respectively ($kg\text{-}m^2$)
I_{xy}, I_{xz}, I_{yz}	product of inertia in the XY, XZ and YZ plane, respectively ($kg\text{-}m^2$)
J	cost function
K_β	scale factor
k	general index
m	aircraft mass (kg)
N	number of data points
p, q, r	roll, pitch and yaw rates ($rad\text{-}s^{-1}$)
$\mathbf{R}$	measurement covariance matrix
S_w	wing planform area (m^2)
T	temperature (K)
t	time (s)
u, v, w	longitudinal, lateral and vertical airspeed components, respectively (ms^{-1})
V	airspeed (ms^{-1})
Y, Z	estimated and measured output, respectively
α, β	angle-of-attack and angle-of-slide-slip, respectively (deg)
Δ	bias (m)
$\delta_a, \delta_e, \delta_r$	aileron, elevator and rudder deflection angles, respectively (deg)
ε	error
ϕ, θ, ψ	angles of roll, pitch and yaw, respectively (deg)
ρ	density ($kg\text{-}m^{-3}$)
Θ	vector of unknown parameters

Subscripts

m	measured variables

Superscript

.	time rate of variable

https://doi.org/10.1017/S0001924000010149 Published online by Cambridge University Press

Lateral-directional aerodynamic (stability and control) derivatives

$C_{Y_\beta} = \partial C_Y / \partial \beta$, $C_{l_\beta} = \partial C_l / \partial \beta$, $C_{n_\beta} = \partial C_n / \partial \beta$

$C_{Y_p} = \partial C_Y / \partial (pb/2u)$, $C_{l_p} = \partial C_l / \partial (pb/2u)$, $C_{n_p} = \partial C_n / (\partial (pb/2u))$

$C_{Y_r} = \partial C_Y / \partial (rb/2u)$, $C_{l_r} = \partial C_l / \partial (rb/2u))$, $C_{n_r} = \partial C_n / (\partial (rb/2u))$

$C_{Y_{\delta_r}} = \partial C_Y / \partial \delta_r$, $C_{l_{\delta_r}} = \partial C_{l)} / \partial \delta_r$, $C_{n_{\delta_r}} = \partial C_n / \partial \delta_r$

$C_{Y_{\delta_a}} = \partial C_Y / \partial \delta_a$, $C_{l_{\delta_a}} = \partial C_l / \partial \delta_a$, $C_{n_{\delta_a}} = \partial C_n / \partial \delta_a$

1.0 INTRODUCTION

The process of aircraft parameter (aerodynamic or stability and control derivatives) estimation involves the determination of best possible estimates of the parameters occurring in the model used to represent it. The parameter estimation[1-16] from real flight data is a routine task for many aerospace organisations. Although reasonably accurate parameters can be obtained through analytical predictions and wind tunnel testing, the parameter estimation using flight data help to enhance the confidence in the estimates significantly. Designing optimal controls and autopilots, expansion of flight envelopes, updating simulators and verification of overall aircraft performance are some of the uses of parameter estimation.

The conventional methods (output error methods[1-5,11-12] and its variants such as least squares[1-2,11-12] and maximum likelihood[1,3-5,11-12] methods) require an a priori postulation of correct flight dynamic formulations having accurate and exact description of aerodynamic model for identification (parameter estimation) from flight data. The most of the conventional estimation methods find it difficult to handle flight data having reasonable amount of process noise (modelling error).

Recently, investigations have been carried out to explore the potential of artificial neural networks[6-16] for aircraft aerodynamic modeling and parameter estimation. Feed forward neural network (FFNN) is found to be the most promising for its application to aircraft modeling. The strength of FFNN lies in its ability to capture highly nonlinear complex phenomena for which the model postulation with physical understanding is difficult. It has been shown that FFNN[12] can work as general function approximators and, thereby, are capable of approximating any continuous function to any desired accuracy provided the appropriate neural architecture is chosen. In the present work, neural Gauss-Newton[14-16] method, proposed by Peyada[14], has been used for aerodynamic parameter estimation from real flight data. The neural Gauss-Newton (NGN) method maps the input/output measurements of the system directly and utilises the ability of FFNN to model any nonlinear continuous function without going into the physical details of the network while handling the problem of process noise.

The conventional (LS and ML) and neural based method (NGN) are shown to adequately estimate lateral-directional aerodynamic parameters from lateral-directional real flight data. The lateral-directional flight data was gathered during the flight testing of Hansa-3 aircraft by executing manoeuvers using lateral-directional control inputs. It could be observed from the results that all the estimation methods gave aerodynamic parameters with reasonably good accuracy. The non-requirement of a priori mathematical model along with adequate estimation, in case of NGN method, is an additional advantage. The paper also presents the effect of type of control input on the estimation. The validation has been done by carrying out the proof-of-match exercise.

In the presented study, Section 2.0 presents the process of gathering real flight data during flight testing using Hansa-3 aircraft. Data compatibility check to make the data compatible for

https://doi.org/10.1017/S0001924000010149 Published online by Cambridge University Press



Figure 1. The Hansa-3 research aircraft.

estimation has been presented in Section 3.0. In Section 4.0, mathematical/aerodynamic model for lateral-directional case has been presented. Section 5.0 presents the estimation of aerodynamic derivatives using conventional and neural-based methods along with results and discussion. The concluding remarks have been highlighted in Section 7.0.

2.0 GENERATION OF REAL FLIGHT DATA

A flight test program using the Hansa-3[16] (Fig. 1), an in-house fully instrumented research aircraft, was conducted at Flight Laboratory of Indian Institute of Technology, Kanpur (India) to gather the real flight data with the help of a data acquisition system. Although a large number of lateral-directional flight data sets were gathered during flight testing, ten data sets were used to estimate lateral-directional aerodynamic parameters using conventional and neural-based estimation methods.

The Hansa-3 aircraft has been manufactured by the National Aerospace Laboratories, India and instrumented with a wide range of sensors for acquisition of flight data for the research purposes. The Hansa-3 test aircraft is an all composite, two-seater trainer airplane. The aircraft is equipped with dual control system. It has a low cantilever wing with side-by-side seating arrangement. The landing gear is of tricycle (nose-wheel) configuration. A turbocharged Rotax-914 F3 engine is fitted to the aircraft. A Hoffmann propeller is coupled to the four-stroke, four-cylinder, horizontally opposed, spark ignition Rotax engine.

An onboard measurement system installed on test aircraft provided the measurements using dedicated sensors for a large number of signals such as aircraft motion variables, atmospheric conditions, control surface deflections, etc. The measurements made in flight were recorded on board at a sampling rate of 50Hz using a suitable interface with a standard laptop computer. The tests were conducted at thrust of 1,200N approximately.

The flight tests in lateral-directional case were conducted at 4,000ft, 6,000ft and 8,000ft altitudes. The ten sets of lateral-directional flight data were acquired by executing aileron/rudder control input deflections for the estimation of lateral-directional aerodynamic parameters using conventional and neural-based estimation methods. Figures 2 to 11 present the ten sets of processed lateral-directional flight data such as HLD1, HLD2, HLD3 … HLD10 in graphical form in terms of the motion variables. The lateral-directional control surfaces were deflected either simultaneously or separately. The ailerons and rudder were actuated simultaneously to generate three data sets HLD1, HLD2 and HLD3. The ailerons were actuated while keeping rudder at trim condition to generate HLD4 and HLD5. The rudder was actuated while keeping ailerons at trim condition to generate HLD6, HLD7, HLD8, HLD9 and HLD10.

https://doi.org/10.1017/S0001924000010149 Published online by Cambridge University Press

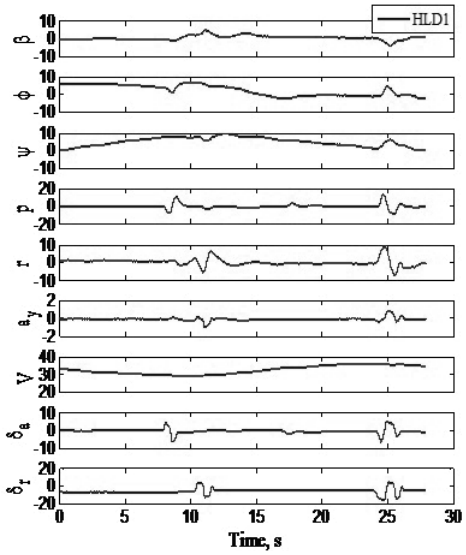


Figure 2. Flight data using aileron-rudder actuation: HLD1.

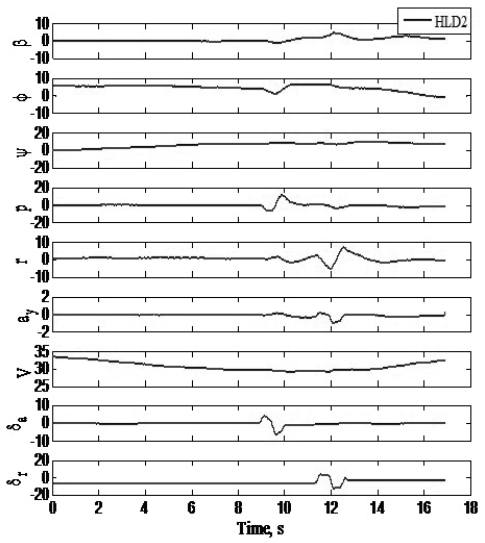


Figure 3. Flight data using aileron-rudder actuation: HLD2.

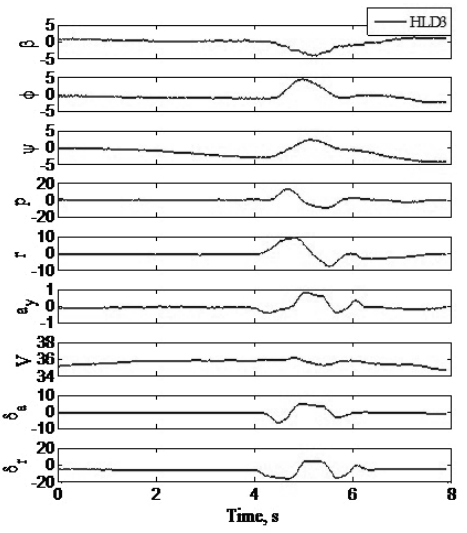


Figure 4. Flight data using aileron-rudder actuation: HLD3.

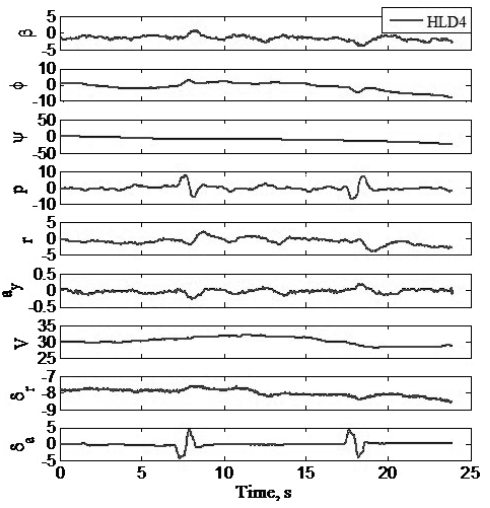


Figure 5. Flight data using aileron actuation: HLD4.

Figures 2 to 11 present the variation of lateral-directional motion variables such as angle of sideslip (β), roll angle (ϕ), yaw angle (ψ), roll rate (p), yaw rate (r), linear acceleration (a_y) along y-axis and velocity (V) pertaining to doublet aileron and/or rudder (δ_a and/or δ_r) control inputs. For the sake of more clarity, the units of variables have not been mentioned in the figures used to represent flight data. It is to mention that the variables such as α, β, ϕ, θ, ψ, δ_a, δ_e and δ_r are in degree

https://doi.org/10.1017/S0001924000010149 Published online by Cambridge University Press

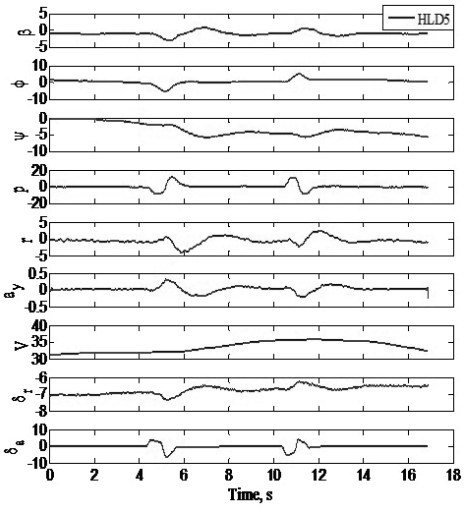


Figure 6. Flight data using aileron actuation: HLD5.

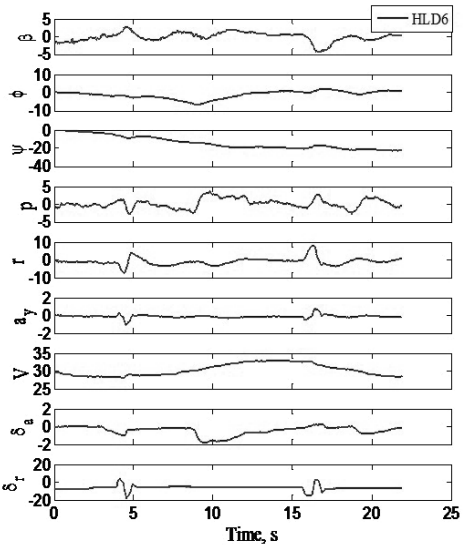


Figure 7. Flight data using rudder actuation: HLD6.

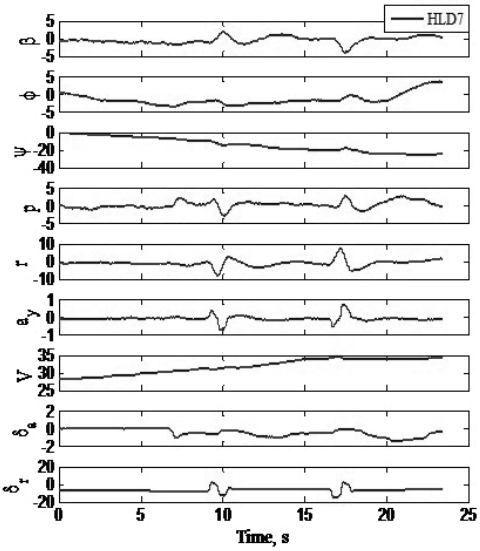


Figure 8. Flight data using rudder actuation: HLD7.

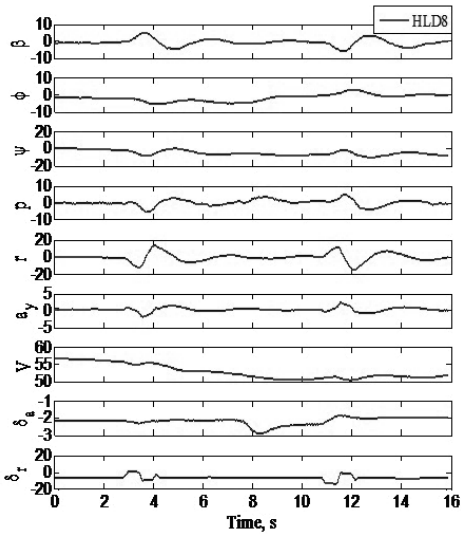


Figure 9. Flight data using rudder actuation: HLD8.

whereas the variables a_x, a_y and a_z are in ms^{-2}. The variables p, q and r are in degree/s. Velocity vector, **V** is in ms^{-1}. The units of state and motion variables mentioned above are applicable to all the figures presented throughout the work presented in this paper.

In the terminology used to define the data sets such as HLD1, HLD2, etc, the term 'H' stands for 'Hansa-3 aircraft', 'LD' stands for 'lateral-directional' and the numerals '1, 2, ... 10' define

https://doi.org/10.1017/S0001924000010149 Published online by Cambridge University Press

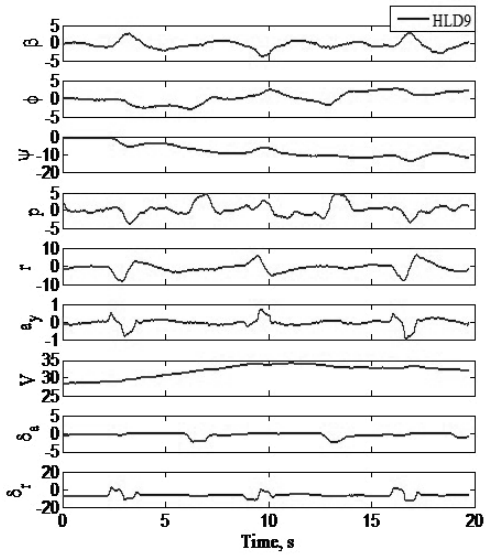


Figure 10. Flight data using rudder actuation: HLD9.

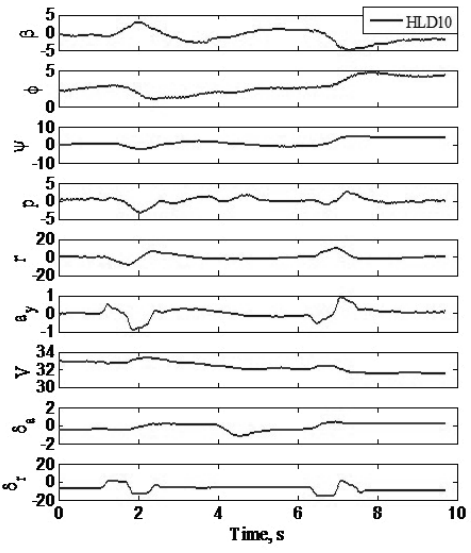


Figure 11. Flight data using rudder actuation: HLD10.

the number of data sets. The aileron and/or rudder control surfaces were deflected from the trim condition to generate the lateral-directional flight data at various speeds. It can be seen that the trim angle for aileron and rudder are approximately zero and −7 degrees, respectively for most of the cases. The values of ψ, p, r and a_y corresponding to trim condition can be observed to be zero. The trim value of β can be observed to be approximately zero for most of the cases except for the flight data HLD3, HLD4 and HLD6. The trim value of β can also be observed to be approximately zero for most of the cases except for the flight data HLD1, HLD2 and HLD10. Although, the velocity was varied between 28ms^{-1} to 57ms^{-1} but, most of the time it was kept around 30ms^{-1}.

It can also be observed that the lateral variables (ϕ, p) were affected when the ailerons were deflected from trim condition whereas the rudder deflection affects the directional variables (β, r). A positive increase in aileron deflection from trim condition results in negative roll rate and reduction in bank angle whereas a positive increase in rudder deflection results in negative yaw rate and positive angle of sideslip. A coupling effect can also be observed i.e. lateral and directional variables were also affected slightly when the control deflections were actuated through directional and lateral controls, respectively.

3.0 DATA COMPATIBILITY CHECK

The recorded real flight data are mainly corrupted by systematic errors like scale factors, zero shift biases and time shifts. These errors introduce data incompatibility; for example, data incompatibility would exist by way of the measured incidence angles not being in agreement with those reconstructed from the accelerometer and rate gyro measurements. In the context of aerodynamic characterisation of an aircraft, a large number of variables are usually measured and recorded during flight test programme. Thus, it is imperative that the data compatibility check is carried out before using the data for aerodynamic modeling and parameter estimation.

https://doi.org/10.1017/S0001924000010149 Published online by Cambridge University Press

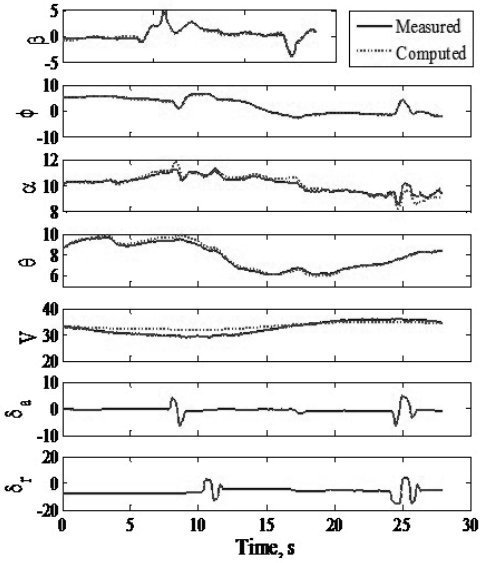


Figure 12. Data compatibility check: HLD1.

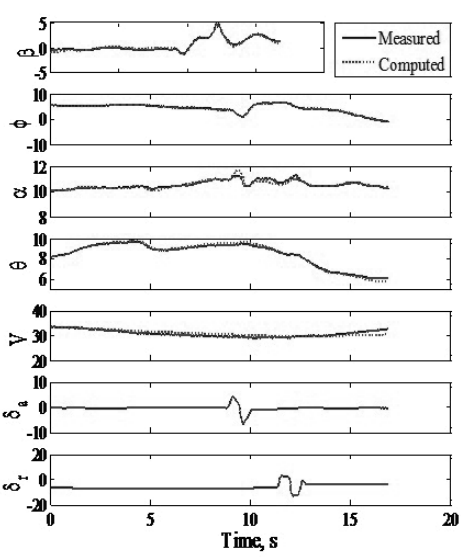


Figure 13. Data compatibility check: HLD2.

In other words, the data compatibility check, which is also called as flight path reconstruction[12] (FPR), is an integral part of aircraft parameter estimation. The main aim of a data compatibility check is to ensure that the measurements used for subsequent aerodynamic model identification are consistent and error free (as far as possible). For example, the measured angle-of-attack and angle-of-sideslip must match with those reconstructed from the measured linear accelerations and angular rates. Such verification is possible in the case of flight data because the well-defined kinematic equations of aircraft motion provide a convenient means to bootstrap the information through a numerical procedure[12]. The kinematic equations are composed of equations of translational motion, the rotational kinematic equations and the navigation equations in body fixed axes. For the purpose of simplification, it is assumed that the aircraft is a rigid body. The mathematical model used for the data compatibility check is described by the three sets of kinematic equations (translational, rotational and navigation) in the body fixed axes[12].

The data compatibility check was carried out on ten sets of flight data (HLD1 … HLD10) pertaining to lateral-directional case using observation equations and the ML method. Figures 12 to 13 present the measured and computed response of motion variables such as β, φ, α, θ and V obtained during the data compatibility check for the flight data sets HLD1 and HLD2. Similar response was obtained in case of other data sets. The units of motion variables used to express the graphical presentations are same as explained earlier.

It can be observed from Figs 12 and 13 that the computed response compares well with the measured response for most of the motion variables (α, θ, β and φ). A similar trend in the variation of velocity was observed in lateral-directional case also.

Equation (1) represents the unknown parameter vector (Θ) that consists of scale factor (K_β) and biases ($\Delta a_x \Delta a_y \Delta a_z \Delta p \Delta q \Delta r \Delta\beta$) and is considered adequate for reconstructing lateral-directional dynamics of Hansa-3 aircraft.

$$\Theta = [\Delta a_x \Delta a_y \Delta a_z \Delta p \Delta q \ \Delta r \ K_\beta \Delta\beta]^T \quad \ldots (1)$$

https://doi.org/10.1017/S0001924000010149 Published online by Cambridge University Press

Table 1
Data compatibility check: Lateral-directional flight data

Factors → Input ↓	Δa_x (ms^{-2})	Δa_y (ms^{-2})	Δa_z (ms^{-2})	Δp (rad/s)	Δq (rad/s)	Δr (rad/s)	K_β	$\Delta\beta$ (rad)
HLD1	0·2478	0·1827	0·083	–0·0006	–0·0011	0·0023	1·0167	–0·0122
	(0·0023)	0·0009)	(0·0005)	0·0000)	(0·0000)	(0·0000)	(0·0005)	(0·0002)
HLD2	0·4557	0·2303	0·1257	–0·0007	–0·0008	0·0018	1·0804	–0·0141
	(0·0027)	(0·0015)	(0·0006)	(0·0000)	(0·0000)	(0·0000)	(0·0102)	(0·0003)
HLD3	0·1730	0·1649	0·0201	–0·0002	–0·0008	0·0021	0·9816	–0·0041
	(0·0030)	(0·0034)	(0·0011)	(0·0000)	(0·0000)	(0·0000)	(0·0094)	(0·0004)
HLD4	0·0763	0·2846	0·0128	0·0003	–0·0002	0·0032	0·8392	–0·0102
	(0·0017)	(0·0013)	(0·0005)	(0·0000)	(0·0000)	(0·0000)	(0·0175)	(0·0003)
HLD5	–0·0587	0·3128	–0·0041	0·0005	–0·0011	–0·0026	0·9497	0·0016
	(0·0022)	(0·0009)	(0·0004)	(0·0000)	(0·0000)	(0·0000)	(0·0099)	(0·0003)
HLD6	0·2134	0·1867	0·0297	0.0007	–0·0005	0·0005	1·0340	–0·0072
	(0·0024)	(0·0013)	(0·0006)	(0·0000)	(0·0000)	(0·0000)	(0·0109)	(0·0004)
HLD7	0·1628	0·2346	0·0449	0·0007	–0·0005	–0·0005	0·8619	0·0086
	(0·0009)	(0·0012)	(0·0005)	(0·0000)	(0·000)	(0·0000)	(0·0104)	(0·0004)
HLD8	0·3072	0·4767	–0·0364	–0·0004	0·0001	0·0029	0·9861	0·0050
	(0·0019)	(0·0022)	(0·0009)	(0·0000)	(0·000)	(0·0000)	(0·0048)	(0·0003)
HLD9	–0·0643	0·3750	–0·0010	0·0007	–0·0009	–0·0030	0·9687	0·0079
	(0·0026)	(0·0009)	(0·0007)	(0·0000)	(0·0000)	(0·0000)	(0·0064)	(0·0002)
HLD10	0·2926	0·3321	0·0337	0·0006	–0·0009	–0·003	0·9895	–0·0016
	(0·0016)	(0·0028)	(0·0007)	(0·0000)	(0·0000)	(0·0000)	(0·0060)	(0·0003)

( ) Cramer-Rao bounds

The maximum likelihood method was used to estimate the compatibility factors from flight data pertaining to lateral-directional control inputs. Table 1 presents the values of scale factor (K_β) and biases ($\Delta a_x\ \Delta a_y\ \Delta a_z\ \Delta p\ \Delta q\ \Delta r\ \Delta\beta$) estimated from all the ten sets of lateral-directional flight data.

The values mentioned in parentheses are the Cramer-Rao bounds[12] suggesting the level of accuracy. It can be observed from Table 1 that the biases are negligible and scale factor is close to unity for most of the real flight data sets pertaining to lateral-directional control inputs.

It can also be observed (Table 1) that the values of Cramer-Rao bounds estimated along with compatibility factors are very low. The scale factor close to unity, negligible biases and very low values of Cramer-Rao bounds establish the high accuracy level of the data gathered during the flight testing.

https://doi.org/10.1017/S0001924000010149 Published online by Cambridge University Press

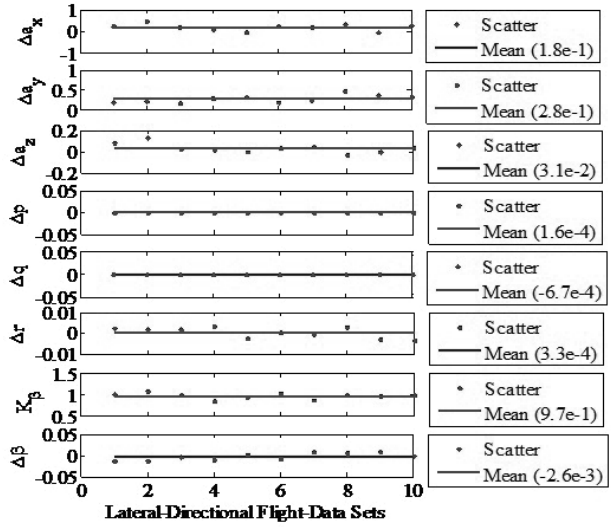


Figure 14. Scatter plot of compatibility factors: Lateral-directional flight data.

Figure 14 presents the scatter plot of estimated compatibility factors about mean value for all the sets of flight data pertaining to lateral-directional control inputs. The fact of high accuracy of gathered data established by the estimated compatibility factors (Table 1) is also evident from the low scatter of compatibility factors about mean value (Fig. 14).

4.0 MATHEMATICAL MODEL

Equations (2) to (5) represent the state equations (simplified case) for lateral-directional case and are used to postulate the aerodynamic model[11-12] for the estimation of lateral-directional parameters.

$$\dot{\beta} = -r + \frac{g}{V}\ \text{Sin}\phi - \frac{\rho V S_w}{2m} C_Y \qquad \ldots (2)$$

$$\dot{p} = \rho V^2\ S_w\ \bar{c}\ \ \frac{(I_Z\ C_1 + \mathrm{I}_{XZ}\ C_n\ )}{2(I_X\ I_Z - I_{XZ}^2)} \qquad \ldots (3)$$

$$\dot{r} = \rho V^2 S_w \bar{c} \frac{(I_X C_n + I_{XZ} C^1)}{2(I_X I_Z - I_{XZ}^2)} \qquad \ldots (4)$$

$$\dot{\varphi} = p \qquad \ldots (5)$$

The side-force coefficient, rolling moment coefficient and yawing moment coefficient appearing in Equations (2) to (4) are modelled as per Equations (6) to (8).

$$C_Y = C_{Y_0} + C_{Y_\beta}\beta + C_{Y_p}\left(\frac{pb}{2V}\right) + C_{Y_r}\left(\frac{rb}{2V}\right) + C_{Y_{\delta_r}}\ \delta_r \qquad \ldots (6)$$

https://doi.org/10.1017/S0001924000010149 Published online by Cambridge University Press

$$C_l = C_{l_0} + C_{l_\beta}\beta + C_{l_p}\left(\frac{pb}{2V}\right) + C_{l_r}\left(\frac{rb}{2V}\right) + C_{l_{\delta_a}}\delta_a + C_{l_{\delta_r}}\delta_r \quad \ldots (7)$$

$$C_n = C_{n_0} + C_{n_\beta}\beta + C_{n_p}\left(\frac{pb}{2V}\right) + C_{n_r}(rb/2V) + C_{n_{\delta_r}}\delta_r \quad \ldots (8)$$

Equation (9) represents the unknown parameter vector (Θ) consisting of lateral-directional aerodynamic derivatives. The aim is to estimate the unknown parameter vector, Θ using the conventional and the neural based methods from the lateral-directional flight data corresponding to the doublet aileron and/or rudder control inputs.

$$\Theta = [C_{Y_0}\ C_{Y_\beta}\ C_{Y_p}\ C_{Y_r}\ C_{Y_{\delta_r}}\ C_{l_0}\ C_{l_\beta}\ C_{l_p}\ C_{l_r}\ C_{l_{\delta_a}}\ C_{l_{\delta_r}}\ C_{n_0}\ C_{n_\beta}\ C_{n_p)}\ C_{n_r}\ C_{n_{\delta_r}}\ C_{n_\beta}]^T \quad \ldots (9)$$

5.0 PARAMETER ESTIMATION

5.1 Parameter estimation using maximum likelihood method

For more than three decades, the maximum likelihood[3,11-12] parameter estimators have been successfully applied for the estimation of the aircraft parameters (stability and control derivatives) using the flight data. The application of the ML method to flight data of an air vehicle requires the postulation of a correct flight dynamic formulations having accurate description of aerodynamic model. The application of the ML method to flight data with either the measurement noise or the process noise has been accepted as a standard approach for the estimation of aircraft aerodynamic parameters. However, in the presence of both (the measurement and the process noise), the ML estimator might lead to the convergence problems and other practical difficulties.

The main advantage of ML method is that the estimates are asymptotically unbiased, consistent and efficient. The method also provides a measure of accuracy in terms of the Cramer-Rao bounds[12] as a part of the ML algorithm.

The cost function is the function of difference between the measured and computed time histories. For no state noise and a known covariance matrix, Equation (10) presents the cost function to be minimised using ML method.

$$J(\Theta) = \tfrac{1}{2}\sum_{i=1}^{N}\left\{[Z(t_i) - Z_\Theta(t_i)]^T\ (GG^T)^{(-1)}\ [Z(t_i) - Z_\Theta(t_i)]\right\} \quad \ldots (10)$$

where N is number of data points, GG^T is measurement noise covariance matrix and $Z_\Theta(t_i)$ is the computed response estimate of Z at t_i for a given value of the unknown parameter vector, Θ. The matrix $\mathbf{GG^T}$ can be approximated by a diagonal matrix.

The compatible lateral-directional flight data sets were used to estimate lateral-directional aerodynamic parameters. The ML method was used to minimise the cost function [$J(\Theta,R)$] to estimate the aerodynamic parameter vector (Θ) given in Equation (9).

Figures 15 to 16 present the measured and estimated response of the motion variables such as angle-of-sideslip (β), bank angle (ϕ), roll rate (p), yaw rate (r), linear acceleration (a_y) along y-body axis obtained during the process of parameter estimation using ML method for the two sets of lateral-directional flight data (HLD1 and HLD2). It can be observed that the measured response matches well with the model estimated response for most of the motion variables (β, φ, p, r and a_y). Similar response was obtained for the other data sets.

https://doi.org/10.1017/S0001924000010149 Published online by Cambridge University Press

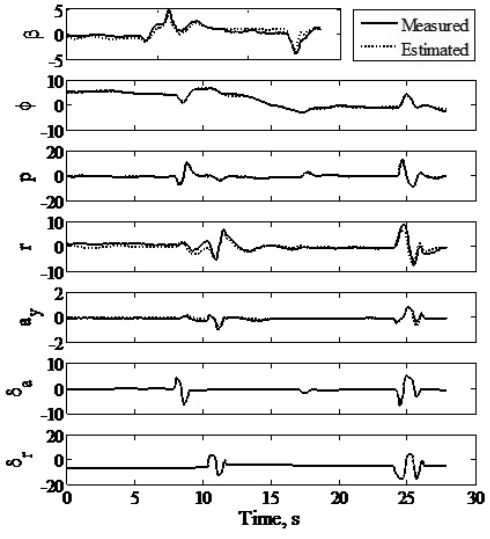


Figure 15. Parameter estimation using ML method: HLD1.

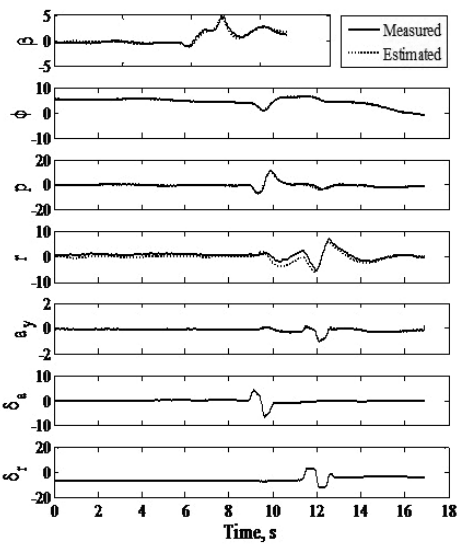


Figure 16. Parameter estimation using ML method: HLD2.

Tables 2 and 3 present the estimated lateral-directional aerodynamic parameters along with their Cramer-Rao bounds[12] obtained from lateral-directional flight data using ML method. The estimated parameters are compared to the wind tunnel estimates (column 2). It can be observed (Tables 2 and 3) that the estimated aerodynamic parameters such as C_{Y_β}, $C_{Y_{\delta_r}}$, C_{l_β}, $C_{l_{(\delta_a)}}$, C_{n_β} and $C_{n_{\delta_r}}$ are consistent and in close agreement with the wind tunnel estimates for most of the lateral-directional flight data sets. The most of the flight data sets gave consistent values of estimated damping C_{l_p} and C_{n_r} and cross C_{l_r} and C_{n_p} derivatives (parameters). The values of aerodynamic parameters such as C_{Y_p} and C_{Y_r} were also consistent for most of the flight data sets. Although the values of estimated parameters such as C_{l_0} and C_{n_0} are having opposite signs in contrast to the wind tunnel estimates, their value is quite small or negligible as desired for most of flight data sets. The aerodynamic parameter C_{Y_0} could not be estimated correctly. The estimated value of the parameter $C_{Y_{\delta_r}}$ was consistent but on a higher side for most of the flight data sets.

It can be observed that the parameters $C_{l_{\delta_r}}$ and $C_{n_{\delta_r}}$ could not be estimated for the data sets HLD4 and HLD5 at all as the rudder deflection was absent during the generation of data. Also, the parameter$C_{l_{\delta_r}}$ could not be estimated correctly for the data sets HLD6, HLD8, HLD9 and HLD10 as absence of aileron deflection in the control input could not generate the required amount of rolling moment. It confirms that the parameter estimated will be incorrect if the data is not having the information content related to estimated parameter.

Figures 17 to 19 present the scatter plot of all the lateral-directional aerodynamic parameters estimated by using ML method from all the ten sets of lateral-directional flight data. Low scatter about the mean value can be observed for most of the aerodynamic parameters. The figures also present the standard deviation about mean value.

https://doi.org/10.1017/S0001924000010149 Published online by Cambridge University Press

Table 2
Parameter estimation using ML method: lateral-directional case

Parameters	WT Value	HLD1	HLD2	HLD3	HLD4	HLD5
C_{Y_0}	−0·013	0·0249	0·0408	0·0347	0·0115	0·0142
		(0·0007)	(0·0009)	(0·0006)	(0·0084)	(0·0035)
C_{Y_β}	−0·531	−0·7108	–0·7144	−0·8205	−0·5561	–0·6295
		(0·0153)	(0·0062)	(0·0105)	(0·0272)	(0·0123)
C_{Y_p}	–	0· 5659	0·4700	0·2535	0·4471	0·3269
		(0·0487)	(0·0276)	(0·0338)	(0·0268)	(0·0139)
C_{Y_r}	–	0·5179	0·9540	0·9634	1·4773	1·0109
		(0·0679)	(0·0281)	(0·0403)	(0·0707)	(0·0342)
$C_{Y_{\delta_r}}$	0·150	0·2838	0·3876	0·3776	0·2027	0·1861
		(0·0062)	(0·0057)	(0·0051)	(0·0645)	(0·0312)
C_{l_0}	0·0015	0·0003	0·0008	−0·0002	–0·0091	−0·0027
		(0·0000)	(0·0000)	(0·0000)	(0·0002)	(0·0001)
C_{l_β}	–0·031	−0·0543	–0·0200	–0·0373	–0·0179	–0·0304
		(0·0009)	(0·0004)	(0·0006)	(0·0013)	(0·0007)
C_{l_p}	–	–0·3259	−0·2562	−0·2965	–0·1683	−0·2547
		(0·0031)	(0·0033)	(0·0040)	(0·0034)	(0·0028)
C_{l_r}	–	0·1376	0·1129	0·1323	0·2282	0·1470
		(0·0034)	(0·0020)	(0·0026)	(0·0066)	(0·0033)
$C_{l_{\delta_a}}$	–0·153	−0·1468	−0·1545	−0·1417	–0·1039	−0·1224
		(0·0012)	(0·0018)	(0·0014)	(0·0014)	(0·0009)
$C_{l_{\delta_r}}$	0·005	0·0117	0·0060	0·0028	–0·0671	−0·0150
		(0·0004)	(0·0005)	(0·0004)	(0·0022)	(0·0010)
C_{n_0}	0·001	−0·0070	–0·0083	−0·0084	−0·0133	–0·0002
		(0·0000)	(0·0001)	(0·0000)	(0·0006)	(0·0001)
C_{n_β}	0·061	0·0654	0·0479	0·0743	0·0859	0·0526
		(0·0006)	(0·0004)	(0·0006)	(0·0016)	(0·0005)
C_{n_p}	–	−0·1961	−0·2190	–0·1817	–0·1515	−0·1419
		(0·0029)	(0·0028)	(0·0026)	(0·0034)	(0·0015)
C_{n_r}	–	−0·1530	–0·0919	−0·1266	−0·0089	−0·1107
		(0·0027)	(0·0021)	(0·0024)	(0·0044)	(0·0023)
$C_{n_{\delta_r}}$	−0·05	−0·0625	–0·0680	–0·0708	–0·1094	–0·0100
		(0·0007)	(0·0007)	(0·0007)	(0·0049)	(0·0013)

( ) Cramer-Rao bounds

5.2 Parameter estimation using least squares method

The least squares (LS) method, also known as regression analysis, is one of the oldest problems in the estimation theory with numerous engineering applications, including flight vehicles. The LS method[2,11-12] assumes the independent variables to be error and noise free and dependent variables corrupted by uniformly distributed noise. The major limitation of these methods is that they yield asymptotically biased and inconsistent estimates in the presence of measurement errors and noise in the independent variables.

https://doi.org/10.1017/S0001924000010149 Published online by Cambridge University Press

Table 3
Parameter estimation using ML method: lateral-directional case

Parameters	WT Value	HLD6	HLD7	HLD8	HLD9	HLD10
C_{Y_0}	−0·013	0·0192	0·0218	0·0330	0·0265	0·0302
		(0·0007)	(0·0006)	(0·0002)	(0·0006)	(0·0004)
C_{Y_β}	−0·531	–0·6601	–0·514	–0·5515	–0·7410	–0·7780
		(0·0142)	(0·0122)	(0·0053)	(0·0130)	(0·0101)
C_{Y_p}	–	0·8117	0·9417	0·7286	0·4683	0·5111
		(0·0817)	(0·0705)	(0·0563)	(0·0524)	(0·1158)
C_{Y_r}	–	0·8424	0·9063	0·5854	0·8844	0·9185
		(0·0537)	(0·0452)	(0·0119)	(0·0319)	(0·0290)
$C_{Y_{\delta_r}}$	0·150	0·2908	0·2866	0·2417	0·3114	0·3309
		(0·0060)	(0·0051)	(0·0022)	(0·0049)	(0·0035)
C_{l_0}	0·0015	−0·0004	−0·0000	–0·0021	–0·0000	–0·0009
		(0·0000)	(0·0000)	(0·0000)	(0·0000)	(0·0000)
C_{l_β}	–0·031	−0·0101	−0·0248	–0·0107	–0·0404	–0·0325
		(0·0003)	(0·0007)	(0·0003)	(0·0014)	(0·0025)
C_{l_p}	–	−0·0781	−0·1935	–0·1117	–0·3192	–0·3527
		(0·0018)	(0·0060)	(0·0040)	(0·0099)	(0·0241)
C_{l_r}	–	0·0819	0·1155	0·0366	0·1224	0·1256
		(0·0019)	(0·0027)	(0·0006)	(0·0034)	(0·0066)
$C_{l_{\delta_a}}$	−0·153	–0·0490	–0·0848	−0·0577	−0·1350	−0·1411
		(0·0009)	(0·0021)	(0·0019)	(0·0037)	(0·0090)
$C_{l_{\delta_r}}$	0·005	–0·0011	0·0054	0·0019	0·0101	–0·0016
		(0·0003)	(0·0003)	(0·0001)	(0·0006)	(0·0004)
C_{n_0}	0·001	–0·0061	–0·0049	–0·0046	–0·0064	–0·0064
		(0·0000)	(0·0000)	(0·0000)	(0·0000)	(0·0000)
C_{n_β}	0·061	0·0646	0·0540	0·0499	0·0670	0·0670
		(0·0007)	(0·0005)	(0·0002)	(0·0006)	(0·0005)
C_{n_p}	–	−0·1353	−0·1223	–0·0770	–0·1574	–0·1149
		(0·0033)	(0·0027)	(0·0028)	(0·0031)	(0·0058)
C_{n_r}	–	–0·0794	−0·0929	–0·0665	–0·1211	–0·0934
		(0·0026)	(0·0024)	(0·0005)	(0·0026)	(0·0015)
$C_{n_{\delta_r}}$	−0·05	–0·0545	−0·0462	–0·0470	–0·0641	−0·0625
		(0·0007)	(0·0006)	(0·0002)	(0·0006)	(0·0005)

( ) Cramer-Rao bounds

The least squares of unknown parameters (Θ) are obtained by minimising the sum of squares of the residuals, or alternatively the weighted sum of squares of the residuals. According to definition, the least-square cost function is defined as:

$$J(\Theta) = \tfrac{1}{2}\, \varepsilon^T \varepsilon = \tfrac{1}{2}\, [Y^T - \Theta^T X^T][Y - X\Theta] \quad \ldots (11)$$

where X and Y are independent and measured dependent variables, respectively and ε is the equation error representing modeling discrepancies and/or noise in the dependent variable.

https://doi.org/10.1017/S0001924000010149 Published online by Cambridge University Press

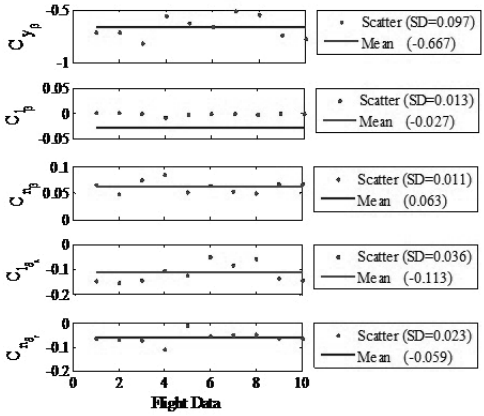


Figure 17. Scatter plot of parameters using ML method.

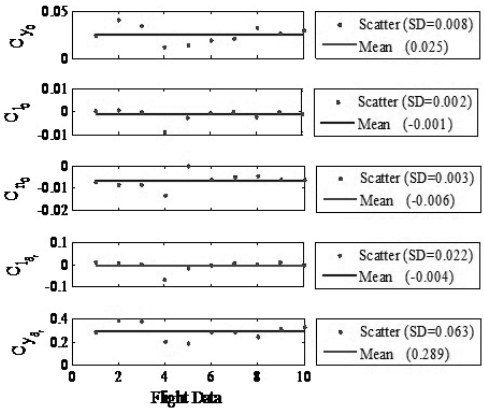


Figure 18. Scatter plot of parameters using ML method.

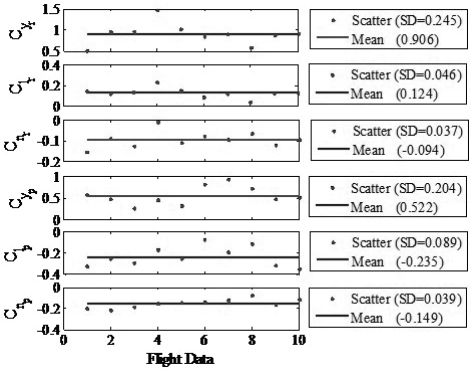


Figure 19. Scatter plot of parameters using ML method.

The LS method was applied to all the ten sets of the lateral-directional flight data (HLD1… HLD10) for the estimation of the lateral-directional aerodynamic parameters. Figures 20 to 21 present the measured and the estimated response of coefficients of aerodynamic force (C_Y) and moments (C_l and C_n) for two sets of lateral-directional flight data (HLD1 and HLD2) obtained during the process of parameter estimation using LS method. It can be observed that the measured response of aerodynamic coefficients matches well with the model estimated response for all the flight data sets. Similar response was obtained for the other data sets.

The parameter vector (Θ) given in Equation (9) was estimated from the compatible real flight data by minimising the cost function [$J(\Theta,R)$] using LS method. Tables 4 and 5 present the estimated lateral-directional aerodynamic parameters along with their Cramer-Rao bounds. The estimated parameters are compared to the wind tunnel estimates (col. 2).

A similar trend in variation of the estimated lateral-directional parameters using LS method, as in case of estimation using ML method, was observed. The estimated aerodynamic parameters such as C_{Y_β},$C_{Y_{\delta_r}}$,C_{l_β},$C_{l_{\delta_a}}$,C_{n_β} and $C_{n_{\delta_r}}$ were consistent and in close agreement with wind tunnel estimates for most of the lateral-directional flight data sets.

https://doi.org/10.1017/S0001924000010149 Published online by Cambridge University Press

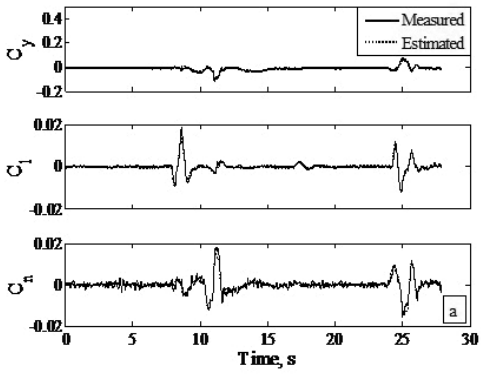


Figure 20. Coefficients estimated using LS method: HLD1.

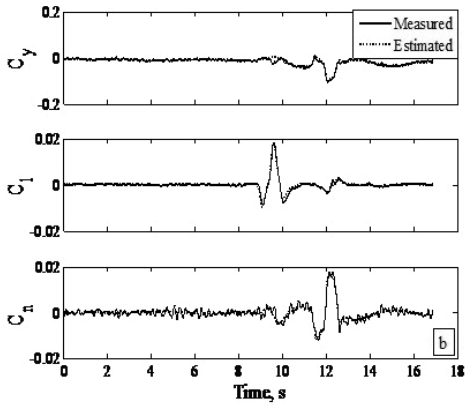


Figure 21. Coefficients estimated using LS method: HLD2.

As in case of estimation using ML method, the aerodynamic parameters such as C_{Y_p}, C_{Y_r}, C_{l_p}, C_{n_r}, C_{l_r} and C_{n_p} most of the flight data sets. Although the values of the estimated parameters such as C_{l_0} and C_{n_0} were having the opposite sign, their value was quite small or negligible as desired for most of the flight data sets.

It can be observed that the parameters$C_{l_{\delta_r}}$ and $C_{n_{\delta_r}}$ could not be estimated for the data sets HLD4 and HLD5 at all as the rudder deflection was absent during the generation of data. Also, the parameter $C_{l_{\delta_a}}$ could not be estimated correctly for the data sets HLD6, HLD8, HLD9 and HLD10 as absence of aileron deflection in the control input could not generate the required amount of rolling moment. It confirms that the parameter estimated will be incorrect if the data is not having the information content related to estimated parameter.

The parameter C_{Y_0} could not be estimated correctly. The estimated value of the parameters $C_{Y\delta_r}$ and $C_{l\delta_r}$ were consistent but on a higher side for most of the flight data sets.

Figures 22 to 24 present the scatter plot of all the lateral-directional aerodynamic parameters estimated through LS method from all the ten sets of lateral-directional flight data. A very low scatter about the mean value can be observed for most of the aerodynamic parameters. The figures also present the standard deviation about mean value.

5.3 Parameter estimation using neural Gauss-Newton method

The Neural Gauss-Newton (NGN) method proposed by Peyada[14] is an algorithm that utilises the feed forward neural network (FFNN) and Gauss-Newton optimisation to estimate the aerodynamic parameters. The neural model has been used to predict the time histories of motion variables at (k+1) th instant given the measured motion variables corresponding to kth instant (where k = 1 to N: N is the total number of discrete data points). For all the practical purposes of parameter estimation, this approach helps in building flight dynamic model (in restricted sense) using measured input-output data and does not require an a priori postulation of the mathematical model or solution of equations of motion.

The algorithm of NGN[14-16] method used to estimate the parameters with the help of block diagram given in Fig. 25 has been summarised below.

https://doi.org/10.1017/S0001924000010149 Published online by Cambridge University Press

Table 4
Parameter Estimation using LS method: Lateral-directional case

Parameters	WT Value	HLD1	HLD2	HLD3	HLD4	HLD5
C_{Y_0}	−0·013	0·0127	0·0194	0·0139	−0·0034	0·0263
		(0·0004)	(0·0011)	(0·0006)	(0·0085)	(0·0052)
C_{Y_β}	−0·531	−0·6491	−0·6185	−0·7207	−0·5328	−0·5183
		(0·0076)	(0·0075)	(0·0099)	(0·0185)	(0·0173)
C_{Y_p}	–	0·1102	0·0239	−0·1901	−0·0520	−0·0721
		(0·0257)	(0·0423)	(0·0320)	(0·0274)	(0·0186)
C_{Y_r}	–	0·6043	0·7021	0·7745	0·2824	0·1457
		(0·0316)	(0·0312)	(0·0429)	(0·0516)	(0·0518)
$C_{Y_{\delta_r}}$	0·150	0·2030	0·2242	0·2374	0·0986	0·2703
		(0·0038)	(0·0076)	(0·0056)	(0·0641)	(0·0459)
C_{l_0}	0·0015	0·0000	0·0010	−0·0002	−0·0121	−0·0050
		(0·0000)	(0·0001)	(0·0)	(0·0019)	(0·0007)
C_{l_β}	−0·031	−0·0371	−0·0218	−0·0384	−0·0203	−0·0283
		(0·0008)	(0·0010)	(0·0010)	(0·0042)	(0·0025)
C_{l_p}	–	−0·2730	−0·2467	−0·2863	−0·2061	−0·2383
		(0·0032)	(0·0062)	0·0041	(0·0070)	(0·0036)
C_{l_r}	–	0·0137	0·0870	0·1398	0·1335	0·1575
		(0·0035)	(0·0040)	(0·0043)	(0·0011)	(0·0079)
$C_{l_{\delta_a}}$	−0·153	−0·1493	−0·1545	−0·1627	−0·1362	−0·1291
		(0·0011)	(0·0022)	0·0014	(0·0023)	(0·0012)
$C_{l_{\delta_r}}$	0·005	0·0107	0·0080	0·0085	−0·0084	−0·0037
		(0·0004)	(0·0010)	(0·0005)	(0·0014)	(0·0068)
C_{n_β}	0·001	−0·0074	−0·0090	−0·0093	−0·0036	−0·0011
		(0·0000)	(0·0002)	(0·0001)	(0·0022)	(0·0012)
C_{n_0}	0·061	0·0635	0·0590	0·0853	0·0546	0·0504
		0·0015	0·0015	(0·0020)	(0·0049)	(0·0042)
C_{n_p}	–	−0·1139	−0·1134	−0·0964	−0·0074	−0·0069
		(0·0052)	(0·0086)	(0·0066)	(0·0073)	(0·0045)
C_{n_r}	–	−0·1110	−0·1215	−0·0902	−0·0022	−0·0321
		(0·0064)	(0·0063)	(0·0089)	(0·0138)	(0·0127)
$C_{n_{\delta_r}}$	−0·05	−0·0685	−0·0774	−0·0814	−0·0354	−0·0166
		(0·0007)	(0·0015)	(0·0011)	(0·0172)	(0·0112)

( ) Cramer-Rao bounds

(a) As a first step, the measured flight data undergoes the data compatibly check. The measured motion variables are then transferred to the centre of gravity for further use during estimation process (Blocks 1-3 of Fig. 25).

(b) The procedure followed for the neural network training using the FFNNs is explained in the blocks 3-8.

(c) The block 9 checks the convergence criteria for the FFNNs training. Once the training is accomplished the trained neural model is used for the parameter estimation.

https://doi.org/10.1017/S0001924000010149 Published online by Cambridge University Press

Table 5
Parameter estimation using LS method: lateral-directional case

Parameters	WT Value	HLD6	HLD7	HLD8	HLD9	HLD10
C_{Y0}	−0·013	0·0073	0·0074	0·0253	0·0014	0·0135
		(0·0004)	(0·0005)	(0·00029)	(0·00045)	(0·0005)
C_{Y_β}	–0·531	–0·5746	−0·4869	−0·5305	−0·5894	−0·5971
		(0·0071)	(0·0081)	(0·0045)	(0·0079)	(0·0076)
C_{Y_p}	–	0·1379	0·5758	0·3169	0·1104	−0·2726
		(0·0425)	(0·0505)	(0·0478)	(0·0347)	(0·0950)
C_{Y_r}	–	0·8531	0·7157	0·5190	0·6871	0·6301
		(0·0263)	(0·0260)	(0·0112)	(0·0206)	(0·0211)
$C_{Y_{\delta_r}}$	0·150	0·1920	0·1606	0·1464	0·1796	0·1742
		(0·0039)	(0·0041)	(0·0025)	(0·0036)	(0·0038)
C_{l_0}	0·0015	0·0005	0·0002	−0·0017	0·0004	0·0001
		(0·0000)	(0·0000)	(0·0001)	(0·0000)	(0·0000)
C_{l_β}	−0·031	−0·02518	−0·0272	−0·0109	–0·0223	–0·0185
		(0·0015)	(0·0012)	(0·0008)	(0·0013)	(0·0017)
C_{l_p}	–	−0·0197	–0·0202	−0·1124	–0·0198	−0·1828
		(0·0105)	(0·0085)	(0·0094)	(0·0081)	0·0166
C_{l_r}	–	0·1080	0·0947	0·0462	0·0960	0·0738
		(0·0039)	(0·0024)	(0·0011)	(0·0032)	(0·0031)
$C_{l_{\delta_a}}$	−0·153	−0·1060	−0·0806	−0·0589	−0·0988	−0·0803
		(0·0053)	(0·0035)	(0·0047)	(0·0033)	(0·0072)
$C_{l_{\delta_r}}$	0·005	0·0089	0·0053	0·0049	0·0088	0·0005
		(0·0005)	(0·0003)	(0·0002)	(0·0005)	(0·0004)
C_{n_0}	0·001	−0·0078	−0·0066	–0·0052	−0·0067	−0·0061
		(0·0001)	(0·0001)	(0·0000)	(0·0001)	(0·0001)
C_{n_β}	0·061	0·0719	0·0694	0·0563	0·0683	0·0664
		(0·0019)	(0·0019)	(0·0009)	(0·0021)	(0·0022)
C_{n_p}	–	−0·0904	−0·0942	−0·0905	−0·1033	−0·1405
		(0·0114)	(0·0123)	(0·0099)	(0·0095)	(0·0278)
C_{n_r}	–	−0·0684	–0·0645	−0·0562	–0·0792	−0·0691
		(0·0070)	(0·0063)	(0·0023)	(0·0057)	(0·0062)
$C_{n_{\delta_r}}$	−0·05	−0·0703	−0·0609	−0·0523	−0·0605	−0·0651
		(0·0010)	(0·0010)	(0·0005)	(0·0010)	(0·0011)

( ) Cramer-Rao bounds

(d) Using the chosen aerodynamic model, the already trained neural model is used to calculate the system output $Y(k)$. The input $U(k)$ is constructed in the block 10 using aerodynamic model fed through block 15. The input $U(k)$ is fed to block 5 to estimate the system output Y(k).

(e) The computed response $Y(k)$ and $\partial Y(k)/\partial\Theta$ (from block 11) are fed to the blocks 12 and 13 to update the aerodynamic parameter. The aerodynamic model is updated using new set of aerodynamic parameters in block 15. The computation through steps (d) to (e) is continued till the convergence criterion (block 14) is achieved. Once the convergence is achieved, aerodynamic parameters are estimated along with associated standard deviation.

https://doi.org/10.1017/S0001924000010149 Published online by Cambridge University Press

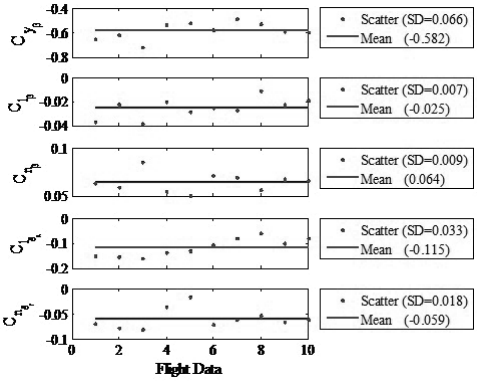


Figure 22. Scatter plot of parameters using LS method.

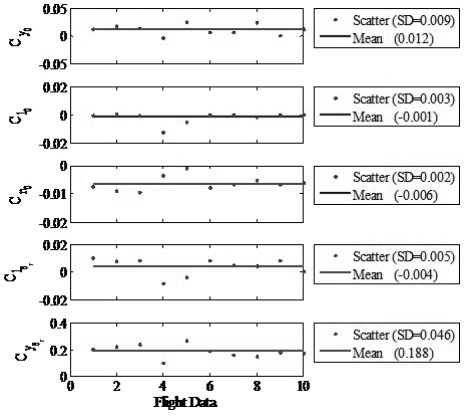


Figure 23. Scatter plot of parameters using LS method.

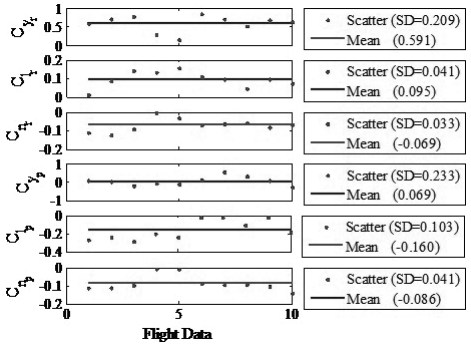


Figure 24. Scatter plot of parameters using LS method.

The NGN algorithm was applied to the ten sets of real lateral-directional flight data (HLD1… HLD10) pertaining to doublet aileron-rudder control inputs. The aim was to estimate the unknown parameter vector Θ [Equation (9)]. Figure 26 presents the neural-architecture for the longitudinal flight dynamic model.

First, the coefficients C_{Y_e}, C_{l_e} and C_{n_e} were computed using the initial guess values of the aerodynamic parameters. Next, the estimated response of the aircraft Y(k+1) at (k+1)th instant was computed using input vector U(k) having same measured flight data with $C_Y(k)$,Cl (k) and $C_n(k)$ replaced by C_{Y_e} ,C_{l_e} and C_{n_e}.

Figures 27 to 28 present the measured and estimated response of aerodynamic coefficients (C_Y, C_l and C_n) obtained during the process of lateral-directional flight dynamic modeling using lateral-directional flight data (HLD1 & HLD2). It can be seen that the measured response of aerodynamic coefficients matches well with the computed response. Similar response was obtained for the other data sets.

https://doi.org/10.1017/S0001924000010149 Published online by Cambridge University Press

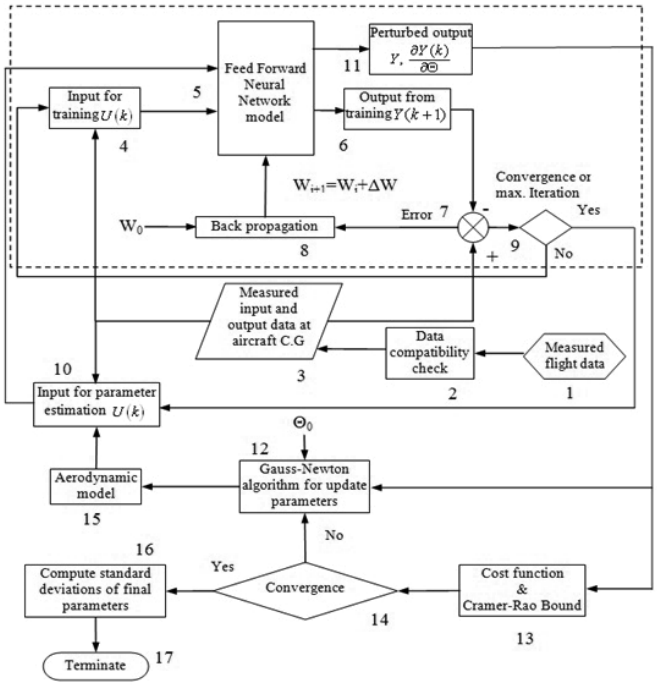


Figure 25. The schematic of NGN method.

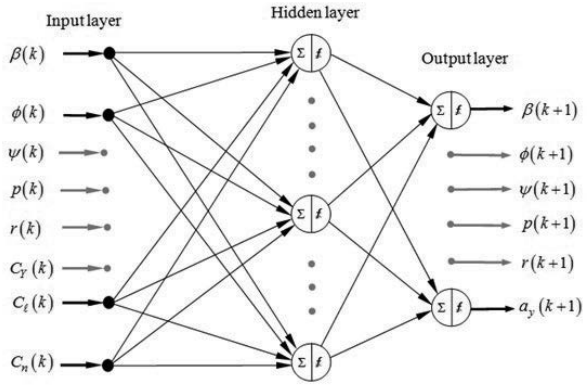


Figure 26. Neural-architecture for lateral-directional flight dynamic model.

The residual error between the measured flight data $Z(k+1)$ and the estimated neural output $Y(k+1)$ was minimised to estimate the unknown parameter vector (Θ). The network parameters varied were the number of hidden layers (1-3), the number of neuron in the hidden layers (2-10), the learning rate (0·1-0·8), the momentum rate (0·1-0·8) and the number of iterations (100-4,000). The network parameters finally chosen gave a good match between true and predicted values of time histories of the variables. The final FFNN structure consisted of one hidden layer having the five neurons with a learning rate of 0·3 and the number of iterations equal to 2,000.

https://doi.org/10.1017/S0001924000010149 Published online by Cambridge University Press

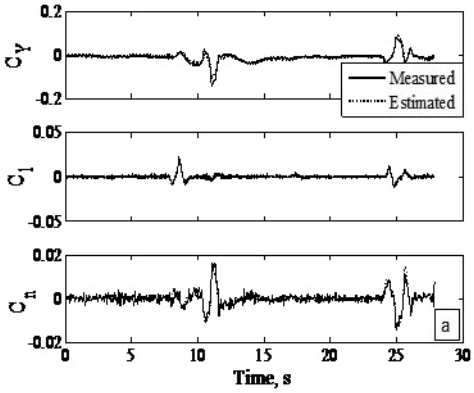


Figure 27. Coefficients using NGN method: HLD1.

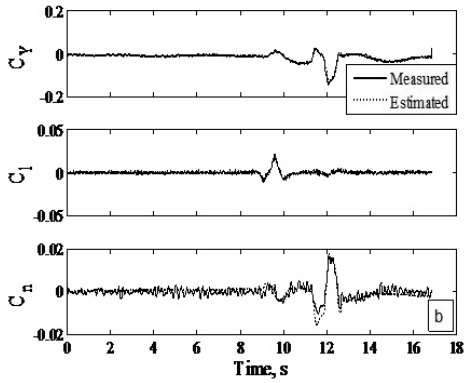


Figure 28. Coefficients using NGN method: HLD2.

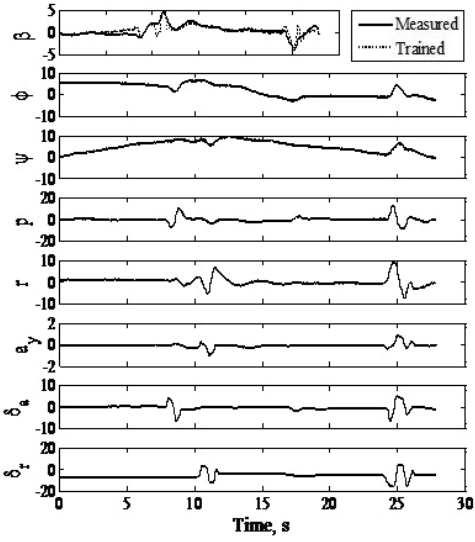


Figure 29. Training using NGN method: HLD1.

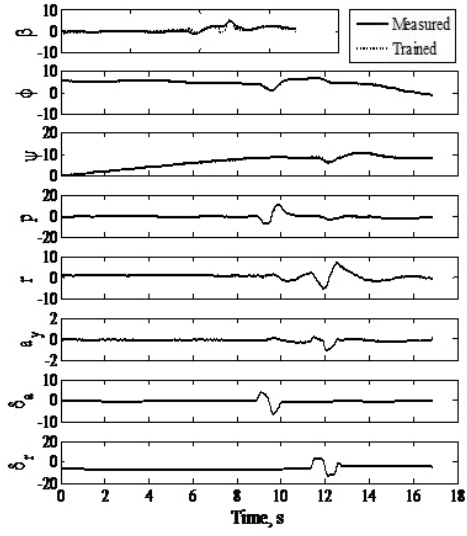


Figure 30. Training using NGN method: HLD2.

The network was trained (using Block 3-8) by varying neural architectural parameters for further estimation of parameters. Figures 29 to 30 present the measured and the trained response of the motion variables such as angle-of-sideslip (β), bank angle (ϕ), yaw angle (ψ), roll rate (p), yaw rate (r) and acceleration (a_y) along y-body axis obtained during the process of training the neural model. It can be observed that the measured response of β, ϕ, ψ, p, r and ay matches well with the trained response for most of the motion variables during the process of neural network model training using all the ten sets of flight data.

The trained network was then used to estimate the parameters. Figures 31 to 32 present the measured and the estimated response of the motion variables such as angle-of-sideslip (β), bank angle (ϕ), yaw angle (ψ), roll rate (p), yaw rate (r) and acceleration (a_y) along y-body axis obtained during the process of parameter estimation from the real lateral-directional flight data sets using the NGN method. Although the estimated coefficients, training and estimation have

https://doi.org/10.1017/S0001924000010149 Published online by Cambridge University Press

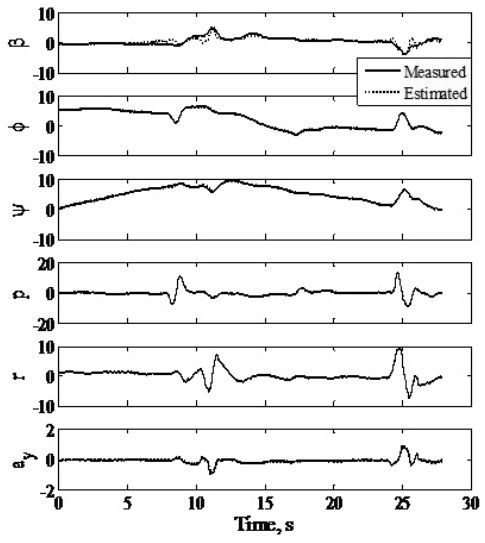


Figure 31. Estimation using NGN method: HLD1.

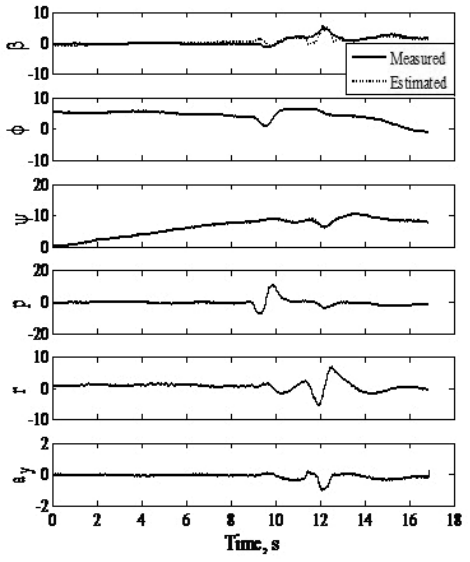


Figure 32. Estimation using NGN method: HLD2.

been presented graphically in three parts, the whole process of estimation was completed in one go. It can be observed that the measured response of β, ϕ, ψ, p, r and ay matches well with the estimated response for most of the motion variables (HLD1 & HLD2).

The parameter vector (Θ) given in Equation (9) was estimated from the compatible real flight data by minimising the cost function [$J(\Theta,R)$] using NGN method. Tables 6 and 7 present the estimated lateral-directional aerodynamic parameters along with their Cramer-Rao bounds. The estimated parameters are compared to the wind tunnel estimates (col. 2). The estimates obtained by using the NGN method were found to be more consistent as compared to the ML and the LS methods. The estimated aerodynamic parameters such as C_{Y_β}, $C_{Y_{\delta_r}}$, C_{l_β}, $C_{l_{\delta_a}}$, C_{n_β} and $C_{n_{\delta_a}}$ were consistent and in close agreement with the wind tunnel estimates for most of lateral-directional flight data sets.

As in case of estimations using ML and LS methods, the aerodynamic parameters such as C_{Y_p}, C_{Y_r}, C_{l_p}, C_{n_r}, C_{l_r} and C_{np} most of the flight data sets. Although the values of the estimated parameters such as C_{l_0} and C_{n_0} were having the opposite sign, their value was quite small or negligible as desired for most of the flight data sets. The aerodynamic parameter C_{Y_0} could not be estimated correctly. The estimated value of the parameters$C_{Y_{\delta_r}}$ and $C_{l_{\delta_r}}$ were consistent but on a higher side for most of the flight data sets.

It can be observed that the parameters$C_{l_{\delta_r}}$ and $C_{n_{\delta_r}}$ could not be estimated for the data sets HLD4 and HLD5 at all as the rudder deflection was absent during the generation of data. Also, the parameter $C_{l_{\delta_r}}$ could not be estimated correctly for the data sets HLD6, HLD8, HLD9 and HLD10 as absence of aileron deflection in the control input could not generate the required amount of rolling moment. It confirms that the parameter estimated will be incorrect if the data is not having the information content related to estimated parameter

Figures 33 to 35 present the scatter plot of all the lateral-directional aerodynamic parameters estimated by using NGN method from all the ten sets of lateral-directional flight data. Low scatter about the mean value can be observed for most of the aerodynamic parameters.

https://doi.org/10.1017/S0001924000010149 Published online by Cambridge University Press

Table 6
Parameter estimation using NGN method: lateral-directional case

Parameters	WT Value	HLD1	HLD2	HLD3	HLD4	HLD5
C_{Y_0}	–0·013	0·0168	0·0298	0·0154	0·0115	0·1042
		(0·0003)	(0·0005)	(0·0006)	(0·0084)	(0·0035)
C_{Y_β}	−0·531	−0·8096	−0·8975	−0·6154	–0·5561	−0·6295
		(0·0063)	(0·0076)	(0·0156)	(0·0272)	(0·0123)
C_{Y_p}	–	0·1825	0·0375	–0·0004	0·4471	0·3269
		(0·0219)	(0·0248)	(0·0001)	(0·0268)	(0·0139)
C_{Y_r}	–	0·6598	1·3262	0·0002	1·4773	1·0109
		(0·0273)	(0·0350)	(0·0001)	(0·0707)	(0·0342)
$C_{Y_{\delta_r}}$	0·150	0·2254	0·3733	0·2021	0·2027	0·1861
		(0·0031)	(0·0044)	(0·0049)	(0·0645)	(0·0312)
C_{l_0}	0·0015	0·0007	0·0012	0·0008	−0·0091	–0·0027
		(0·0001)	(0·0002)	(0·0002)	(0·0002)	(0·0001)
C_{l_β}	–0·031	−0·0290	−0·0253	−0·0394	0·0179	–0·0304
		(0·0021)	(0·0032)	(0·0047)	(0·0013)	(0·0007)
C_{l_p}	–	−0·2865	–0·3056	0·0000	– ·1683	−0·2547
		(0·0088)	(0·0137)	(0·0000)	(0·0034)	(0·0028)
C_{l_r}	–	0·1610	0·1815	0·0000	0·2282	0·1470
		(0·0091)	(0·0141)	(0·0000)	(0·0066)	(0·0033)
$C_{l_{\delta_a}}$	−0·153	−0·1549	−0·1760	−0·1258	–0·1039	−0·1224
		(0·0029)	(0·0046)	(0·0054)	(0·0014)	(0·0009)
$C_{l_{\delta_r}}$	0·005	0·0202	0·0252	0·0218	−0·0671	−0·0150
		(0·0011)	(0·0017)	(0·0021)	(0·0022)	(0·0010)
C_{n_0}	0·001	−0·0076	–0·0109	−0·0042	–0·0133	−0·0002
		(0·0001)	(0·0001)	(0·0002)	(0·0006)	(0·0001)
C_{n_β}	0·061	0·0323	0·0462	0·0495	0·0859	0·0526
		(0·0021)	(0·0029)	(0·0056)	(0·0016)	(0·0005)
C_{n_p}	–	−0·1548	−0·1427	0·0001	–0·1515	−0·1419
		(0·0072)	(0·0096)	(0·0000)	(0·0034)	(0·0015)
C_{n_r}	–	−0·1431	−0·1654	–0·0001	–0·0089	−0·1107
		(0·0092)	(0·0131)	(0·0000)	(0·0044)	(0·0023)
$C_{n_{\delta_r}}$	−0·05	–0·0727	−0·0997	−0·0442	–0·1094	–0·0100
		(0·0010)	(0·0016)	(0·0018)	(0·0049)	(0·0013)

( ) Cramer-Rao bounds

5.4 Validation

To gain more confidence in the methods used, the proof-of-match[7] exercise was carried out for validation of the aerodynamic model. For this, two sets of longitudinal flight data were used for model verification. The predictive capability of the identified model is determined by comparing the flight measured response with those predicted by the model for the same ('identical') control inputs. In flight vehicle applications terminology, this process is often called 'proof-of-match'. It is important part of flight simulator certification and acceptance. In this proof-of-match process, the identified (aerodynamic) model is kept fixed.

https://doi.org/10.1017/S0001924000010149 Published online by Cambridge University Press

Table 7
Parameter Estimation using NGN method: lateral-directional case

Parameters	WT Value	HLD6	HLD7	HLD8	HLD9	HLD10
C_{Y_0}	–0·013	0·0192	0·0218	0·0330	0·0265	0·0302
		(0·0007)	(0·0006)	(0·0002)	(0·0006)	(0·0004)
C_{Y_β}	–0·531	–0·6601	–0·5142	–0·5515	–0·7410	–0·7780
		(0·0142)	(0·0122)	(0·0053)	(0·0130)	(0·0101)
C_{Y_p}	–	0·8117	0·9417	0·7286	0·4683	–0·5111
		(0·0817)	(0·0705)	(0·0563)	(0·0524)	(0· 1158)
C_{Y_r}	–	0·8424	0·9063	0·5854	0·8844	0·9185
		(0·0537)	(0·0452)	(0·0119)	(0·0319)	(0·0290)
$C_{Y_{\delta_r}}$	0·150	0·2908	0·2866	0·2417	0·3114	0·3309
		(0·0060)	(0·0051)	(0·0022)	(0·0049)	(0·0035)
C_{l_0}	0·0015	–0·0004	–0·0000	–0·0021	–0·0000	–0·0009
		(0·0000)	(0·0000)	(0·0000)	(0·0000)	(0·0000)
C_{l_β}	–0·031	–0·0101	–0·0248	–0·0107	–0·0404	–0·0325
		(0·0003)	(0·0007)	(0·0003)	(0·0014)	(0·0025)
C_{l_p}	–	–0·0781	–0·1935	–0·1117	–0·3192	–0·3527
		(0·0018)	(0·0060)	(0·0040)	(0·0099)	(0·0241)
C_{l_r}	–	0·0819	0·1155	0·0366	0·1224	0·1256
		(0·0019)	(0·0027)	(0·0006)	(0·0034)	(0·0066)
$C_{l_{\delta_a}}$	–0·153	–0·0490	–0·0848	–0·0577	–0·1350	–0·1411
		(0·0009)	(0·0021)	(0·0019)	(0·0037)	(0·0090)
$C_{l_{\delta_r}}$	0·005	–0·0011	0·0054	0·0019	0·0101	–0·0016
		(0·0003)	(0·0003)	(0·0001)	(0·0006)	(0·0004)
C_{n_0}	0·001	–0·0061	–0·0049	–0·0046	–0·0064	–0·0064
		(0·0000)	(0·0000)	(0·0000)	(0·0000)	(0·0000)
C_{n_β}	0·061	0·0646	0·0540	0·0499	0·0670	0·0670
		(0·0007)	(0·0005)	(0·0002)	(0·0006)	(0·0005)
C_{n_p}	–	–0·1353	–0·1223	–0·0770	–0·1574	–0·1149
		(0·0033)	(0·0027)	(0·0028)	(0·0031)	(0·0058)
C_{n_r}	–	–0·0794	–0·0929	–0·0665	–0·1211	–0·0934
		(0·0026)	(0·0024)	(0·0005)	(0·0026)	(0·0015)
$C_{n_{\delta_r}}$	–0·05	–0·0545	–0·0462	–0·0470	–0·0641	–0·0625
		(0·0007)	(0·0006)	(0·0002)	(0·0006)	(0·0005)

( ) Cramer-Rao bounds

To validate the model, proof-of-match exercise was carried out using two sets of longitudinal real flight data [HDL (Hansa doublet longitudinal) and HMSL (Hansa multi-step longitudinal)]. The estimates obtained through LS, ML and NGN methods using real flight data HDL were used to generate estimated response for elevator input and initial conditions used for generating flight data HMSL. The estimated response was computed by solving equations of motion [six degrees of freedom (6-DOF)]. The estimated response was then compared with flight measured response of HMSL. The result of the proof-of-match exercise is presented in Fig. 36. It may be appreciated that the response of HMSL estimated using the LS, ML and NGN estimates matches closely with the measured flight data of HMSL.

https://doi.org/10.1017/S0001924000010149 Published online by Cambridge University Press

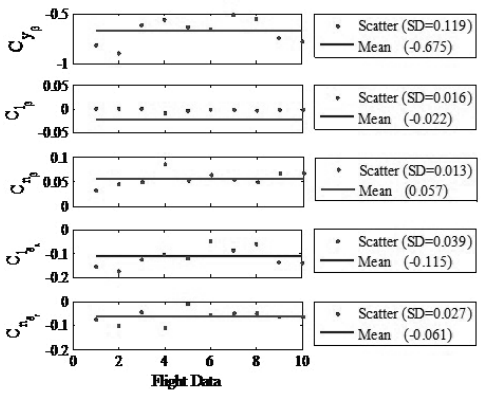


Figure 33. Scatter plot of parameters using NGN method

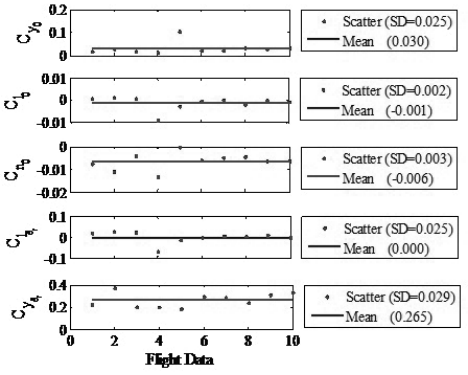


Figure 34. Scatter plot of parameters using NGN method.

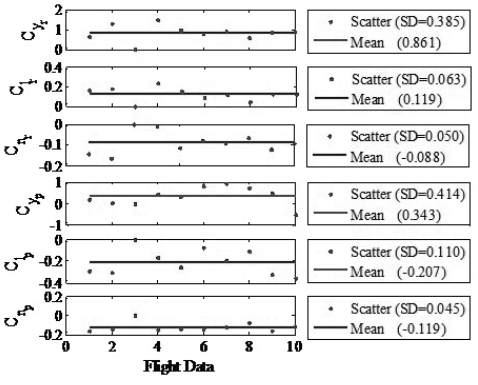


Figure 33. Scatter plot of parameters using NGN method

6.0 CONCLUSION

The main objective of the present work is to provide a consolidated account of flight vehicle system identification using lateral-directional real flight data. The conventional (ML and LS) and neural-based (NGN) methods were used to model the linear aerodynamics using flight data of Hansa-3 aircraft. It was found that NGN method could estimate all the aerodynamic parameters with a reasonable accuracy and the estimates were in close agreement with estimates from conventional methods. The difference lies in the fact that the application of conventional methods for parameter estimation using flight data requires an a priori postulation of correct flight dynamic formulations having accurate description of aerodynamic model where as the NGN method does not require any a priori postulation of mathematical model or solution of equations of motion. The following points were observed during the aerodynamic modeling in time domain.

1. The correct calibration is necessary before the flight test programme to acquire flight data of good quality.

https://doi.org/10.1017/S0001924000010149 Published online by Cambridge University Press

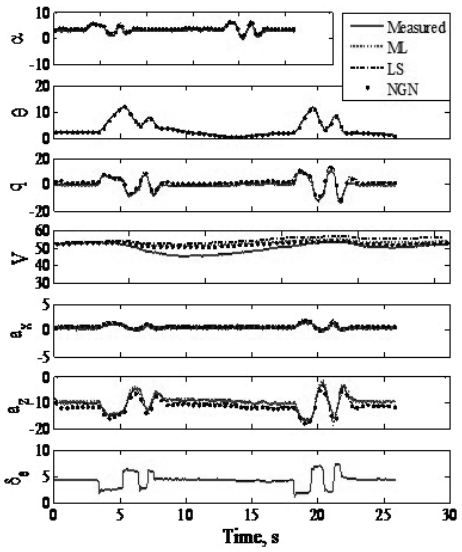


Figure 35. Scatter plot of parameters using NGN method.

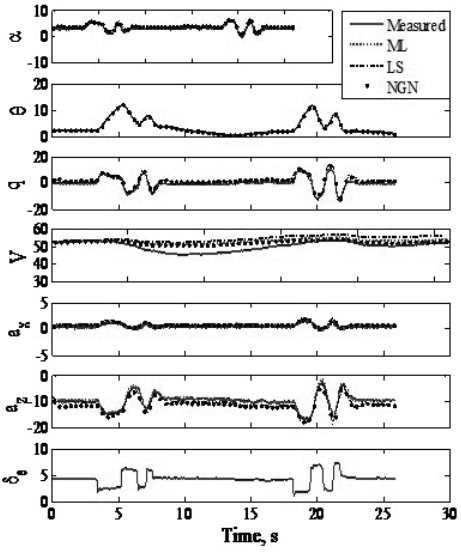


Figure 36. Parameter estimation from HDL and validation using HMSL.

2. The conventional and neural-based methods resulted in satisfactory estimation of most of lateral-directional aerodynamic parameters.
3. Any estimation method (ML, LS or NGN) will give reasonably good estimates of parameters, if real flight data is of good quality and contains the required information contents.
4. The control inputs corresponding to flight data HLD4 and HLD5 affected the estimation of the parameters $C_{l_{\delta_r}}$ and $C_{n_{\delta_r}}$ as these data sets did not have the required information contents for correct estimation.
5. Validation process is necessary to validate the obtained flight data and estimated parameters.

REFERENCES

1. GREENBERG, H. A survey of methods for determining stability parameters of an airplane from dynamic flight measurements, April 1951, NACA TN-2340.
2. SHINBROT, M. A least square curve fitting method with applications to the calculation of stability coefficients from transient response data, April 1951, NACA TN 2341.
3. MEHRA, R.K. Maximum likelihood identification of aircraft parameters, 1970, Proceedings of the 11th Joint Automatic Control Conference, Atlanta, GA.
4. ROSKAM, J. Methods for estimating stability and control derivatives for conventional subsonic airplanes, 1973, Roskam Aviation and Engineering Corporation.
5. MAINE, R.E. and ILIFF, K.W. Identification of dynamic systems — Application to aircraft — Part 1: Output error approach, AGARD-AG-300, December 1986, **3**, (1).
6. YOUSSEF, H.M. and JAUNG, J.C. Estimation of aerodynamic coefficients using neural networks, August 1993, AIAA Paper 93-3639.
7. BASAPPA, K. and JATEGAONKAR, R.V. Aspects of feed forward neural network modeling and its application to lateral-directional flight-data, September 1995, DLR IB 111-95/30.
8. HAMEL, P.G. and JATEGAONKAR, R.V. The evolution of flight vehicle system identification, 8-10 May 1995, AGARD, DLR Germany.

https://doi.org/10.1017/S0001924000010149 Published online by Cambridge University Press

9. RAISINGHANI, S.C., GHOSH, A.K. and KALRA, P.K. Two new techniques for aircraft parameter estimation using neural networks, *Aeronaut J*, January 1998, **102**, (1011), pp 25-29.
10. GHOSH, A.K. Aircraft Parameter Estimation from Flight Data using Feed Forward Neural Networks, April 1998, PhD thesis, Aerospace Engineering Dept, IIT Kanpur.
11. KLEIN, V. and MORELLI, E.A. *Aircraft System Identification — Theory and Practice*, 2006, AIAA Education Series, Reston, VA, USA.
12. JATEGAONKAR, R.V. Flight vehicle system identification — A time domain methodology, *AIAA Progress in Aeronautics and Astronautics*, August 2006, **216**, AIAA, Reston, VA, USA.
13. SINGH, S. Estimation of Aircraft Parameters from Flight Data using Neural Network Based Method, April 2007, PhD thesis, Aerospace Engineering Dept, IIT Kanpur.
14. PEYADA, N.K., and GHOSH, A.K. Aircraft parameter estimation using new filtering technique based on neural network and Gauss-Newton method, *Aeronaut J*, April 2009, **113**, (1142).
15. KUMAR, R. and GHOSH, A.K. Nonlinear longitudinal aerodynamic modeling using neural Gauss-Newton Method, *J Aircr*, September-October 2011, **48**, (5), pp 1809-1812.
16. KUMAR, R. Parameter Estimation Using Flight Data of Air Vehicles at Low and Moderately High Angles of Attack using Conventional and Neural Based Methods, November, 2011, PhD thesis, Aerospace Engineering Department, IIT Kanpur, India.

https://doi.org/10.1017/S0001924000010149 Published online by Cambridge University Press